RSC Chemical Biology



PAPER View Article Online



Cite this: RSC Chem. Biol., 2023, 4 587

Received 5th April 2023, Accepted 2nd June 2023

DOI: 10.1039/d3cb00050h

rsc.li/rsc-chembio

Siderocalin fusion proteins enable a new ⁸⁶Y/⁹⁰Y theranostic approach†

Alexia G. Cosby, Da Trevor Arino, Da Tyler A. Bailey, Da Matthew Buerger, Soshua J. Woods, Da Luis M. Aguirre Quintana, Da Jennifer V. Alvarenga Vasquez, Jennifer N. Wacker, Da Alyssa N. Gaiser, Roland K. Strong and Rebecca J. Abergel Sab

The mammalian protein siderocalin binds bacterial siderophores and their iron complexes through cation- π and electrostatic interactions, but also displays high affinity for hydroxypyridinone complexes of trivalent lanthanides and actinides. In order to circumvent synthetic challenges, the use of siderocalinantibody fusion proteins is explored herein as an alternative targeting approach for precision delivery of trivalent radiometals. We demonstrate the viability of this approach *in vivo*, using the theranostic pair 90 Y (β^- , $t_{1/2}=64$ h)/ 86 Y (β^+ , $t_{1/2}=14.7$ h) in a SKOV-3 xenograft mouse model. Ligand radiolabeling with octadentate hydroxypyridinonate 3,4,3-LI(1,2-HOPO) and subsequent protein binding were achieved at room temperature. The results reported here suggest that the rapid non-covalent binding interaction between siderocalin fusion proteins and the negatively charged Y(III)-3,4,3-LI(1,2-HOPO) complexes could enable purification-free, cold-kit labeling strategies for the application of therapeutically relevant radiometals in the clinic.

The rational chemical design of radiometal-based theranostics relies on (1) pairing the radiological half-life of the radiometal with the biological half-life of the targeting vector; (2) highly kinetically and thermodynamically stable radiometal chelation through rational ligand design; and (3) facile radiolabeling conditions that are amenable to biological targeting vectors, which are often temperature-sensitive.

In this context, the yttrium isotopes 90 Y and 86 Y make an ideal theranostic pair. Yttrium-90 (β^- , β_{ave} = 0.934 MeV, $t_{1/2}$ = 64 hr) is a pure β^- emitter with a multi-day half-life that is highly suitable for use with antibody targeting vectors, which have longer biological half-lives compared to antibody fragments or peptides. The therapeutic potential of this isotope has been highlighted by the clinical approval of Zevalin, 90 Y-ibritumomab-tiuxetan, in 2002, for the treatment of non-Hodgkin lymphoma. This success has prompted further investigation into antibody conjugates incorporating 90 Y.¹

Given the clinical success of ⁹⁰Y-based radiopharmaceuticals, it is advantageous to find a chemically equivalent diagnostic radioisotope to image biodistribution and pharmacokinetics *in vivo*. Yttrium is often treated as a pseudo-lanthanide, owing to its preference to exist in the trivalent oxidation state and comparable ionic radius to those of the lanthanides.² Previous studies have investigated the use of ¹¹¹In, ¹⁷⁷Lu or other substitute diagnostic PET or SPECT isotopes for ⁹⁰Y.³ However, these isotopes can display different coordination chemistry preferences, resulting in release of the metal from the chelator or transchelation by endogenous species *in vivo*.

The positron-emitter, 86 Y (β^+ , $\beta_{ave} = 0.660$ MeV, $t_{1/2} = 14.7$ h), is an ideal diagnostic partner for 90Y, given its chemical equivalence, relieving concern for off-target uptake or in vivo instability. Previous 86/90Y chelation approaches have focused on the non-linear scaffold diethylenetriamine pentaacetate (DTPA)^{4,5} and its derivatives, which allow for rapid complexation kinetics without requiring heat, but at the cost of longterm thermodynamic stability in vivo and leading to increased off-target uptake in healthy tissues. Macrocyclic 1,4,7, 10-tetraazacyclododecane-1,4,7,10-tetraacetic acid (DOTA) has also been used to chelate 86/90Y, but radiolabeling requires elevated temperatures (>90 °C), which are incompatible with heat-sensitive proteins, including antibodies. Efficient use of DOTA thus entails additional processes for targeting vector conjugation as well as subsequent purification steps, in contrast to desired single, cold-kit radiolabeling assembly

^a Chemical Sciences Division, Lawrence Berkeley National Laboratory, Berkeley, CA 94720, USA. E-mail: abergel@berkeley.edu

b Department of Nuclear Engineering, University of California, Berkeley, CA 94720,

^c Division of Basic Sciences, Fred Hutchinson Cancer Center, Seattle, WA 98109, USA

[†] Electronic supplementary information (ESI) available: Experimental, fluorescence quenching, radiolabeling, and PET imaging data. See DOI: https://doi.org/10.1039/d3cb00050h

approaches. The octadentate hydroxypyridinonate chelator 3,4,3-LI(1,2-HOPO), or HOPO, is composed of a spermine backbone and four 1-hydroxypyridin-2-one binding units, and has demonstrated high binding affinity for trivalent (Y(III)-HOPO, $\log \beta_{110} = 20.76$) and tetravalent (Pu(IV)-HOPO, $\log \beta_{110} = 43.1 \pm 0.05$; Th(IV)-HOPO, $\log \beta_{110} = 40.1$) metal ions, including transition, rare earth, and actinide elements.⁶

While ligands such as HOPO may form highly stable complexes in vivo, another requirement for a successful theranostic agent is the incorporation of a targeting vector, which must display a biological half-life compatible with the radiological half-life of the nuclide, and should be synthetically accessible. Antibodies are well-established targeting vectors for cancer therapy. However, despite their clinical utility and ongoing primacy in preclinical theranostic literature, the synthesis of ligands that enable facile chemical conjugation to antibodies often poses a large synthetic challenge. A bifunctional derivative of HOPO incorporating a para-benzyl-isothiocyanate pendant arm was previously synthesized and conjugated to trastuzumab for use with 89Zr for PET imaging.14 Although this conjugate showed promising in vivo stability and significant uptake in tumors, the broader implementation of this construct for therapeutic purposes is likely hampered by its challenging chemical synthesis, which requires 13 steps.

Another conjugation approach is to construct fusion proteins where tyrosine or histidine residues of the antibody or antibody fragment are radioiodinated, such as a 125I-labeled albumin fusion protein construct that showed enhanced uptake in colon carcinoma xenografts.¹⁵ Most fusion protein systems utilize radioiodination of protein tyrosine residues, however these often require harsh chemical reductants and some systems are prone to deiodination in vivo. 16 Additionally, non-specific tyrosyl iodination can also affect antigen binding.

A simpler approach would be to design a fusion protein system that could allow for rapid, room temperature labeling. The mammalian protein siderocalin (Scn) is known to bind bacterial siderophore complexes such as ferric enterobactin (Fe(III)-Ent) through noncovalent, electrostatic interactions $(K_d [Fe(m)-Ent] = 0.4 \text{ nM}$, Table 1), and has also shown selective affinity for HOPO complexes of trivalent lanthanides and actinides, which are negatively charged, in contrast to

Table 1 Summary of M(III/IV)-HOPO stability constants (log β_{110}) and Siderocalin (Scn) dissociation constants (Kd). Superscript denotes reference number

М-НОРО	$\text{Log }\beta_{110} \text{ (stdev)}$	Scn-M-HOPO K _d [nM (stdev)]
Fe(III)-Ent	49 ⁷	0.48
Y(III)-HOPO	$20.76(0.09)^9$	2.4 (0.6) This Work
Sc(III)-HOPO	$25.16(0.09)^9$	5.5(1.1) This Work
Zr(ıv)-HOPO	43.16	No binding
Sm(III)-HOPO	19.7 ¹⁰	13(3) ¹¹
Eu(iii)-HOPO	20.2^{10}	$14(1)^{11}$
Gd(III)-HOPO	$20.5(1)^{10}$	$18(2)^{11}$
Th(iv)-HOPO	40.1 ¹²	No binding
Pu(iv)-HOPO	43.5 ¹²	$110(21)^{11}$
Am(III)-HOPO	$20.4(2)^{13}$	$29(1)^{11}$
Cm(III)-HOPO	$21.8(4)^{13}$	$22(5)^{11}$

corresponding neutral complexes of tetravalent actinides (Table 1).^{6,8,11} Previously, we have capitalized on the high affinity and stability of this interaction to crystallize M(III)-HOPO complexes within the Scn protein, to further confirm the geometric tolerance of the calyx.^{6,11} We hypothesized we could take further advantage of the high affinity interaction between Scn and HOPO complexes to design a radiotheranostic system, where only trivalent radiometals with chemically equivalent theranostic isotopes such as ^{86/90}Y or ^{44/47}Sc are recognized.

A novel approach to circumvent synthetic challenges and exhaustive post-labeling or post-conjugation processes is described herein, through the development of a fusion protein system, where the Scn protein is fused with the HER2+ targeting antibody trastuzumab (IgG-Scn) or a small antibody fragment (Fab-Scn) (Fig. 1). As a theranostic pair, we employ the PET diagnostic isotope 86Y and the therapeutic isotope 90Y for visualization and therapeutic effect in a SKOV-3 xenograft mouse model. Our approach provides the first validation of a theranostic fusion protein system with cold-kit labeling potentially adaptable to a variety of ligand, protein, and radiometal systems.

Results and discussion

We first validated the binding of the HOPO complexes of rare earth Y(III) and Sc(III) within the Scn calyx. Adapting a previously developed method, the dissociation constant or K_d was determined by monitoring the fluorescence quenching of tryptophan ($\lambda_{\text{ex/em}} = 281/380 \text{ nm}$) residues within the protein binding pocket, which is quenched upon recognition of the M-HOPO complex. The results indicate that Y(III)-HOPO and Sc(III)-HOPO both bind rapidly within Scn, with dissociation constants of 2.4 and 5.5 nM respectively (Table 1 and Fig. S2, S3, ESI†). These binding constants are lower than other larger trivalent lanthanides such as Eu(III) or Gd(III) ($K_d = 14$ or 18 nM), potentially indicating a relationship between metal ionic radius and the strength of the noncovalent bonding interactions within the pocket, although studies investigating those trends are on-going. Of note, the decay product of 90Y, 90Zr, is not recognized by the protein, owing to +4 oxidation state of Zr and the overall neutral charge of the corresponding HOPO complex, as indicated by the lack of Scn binding to Zr(IV)-HOPO (Table 1).

Fusion proteins IgG-Scn and Fab-Scn were recombinantly expressed as reported previously, with Scn moieties fused to the antibody heavy chain C-termini. 17,18

The final 86/90Y-HOPO protein constructs (protein = Scn, Fab-Scn, or IgG-Scn) were assembled in two steps. In short, HOPO was dissolved in DMSO and 90YCl3 or 86YCl3 was added at a 1:100 (M:HOPO) molar ratio, followed by incubation at room temperature for 5 minutes. Solutions were further diluted with 1X DPBS and a pH of 7.4 was confirmed by spotting onto pH paper. Subsequently, the 86Y-HOPO or 90Y-HOPO solution was added to 200 equivalents of wildtype Scn, Fab-Scn, or IgG-Scn fusion proteins in a PBS matrix and then incubated at room temperature for an additional 5 minutes.

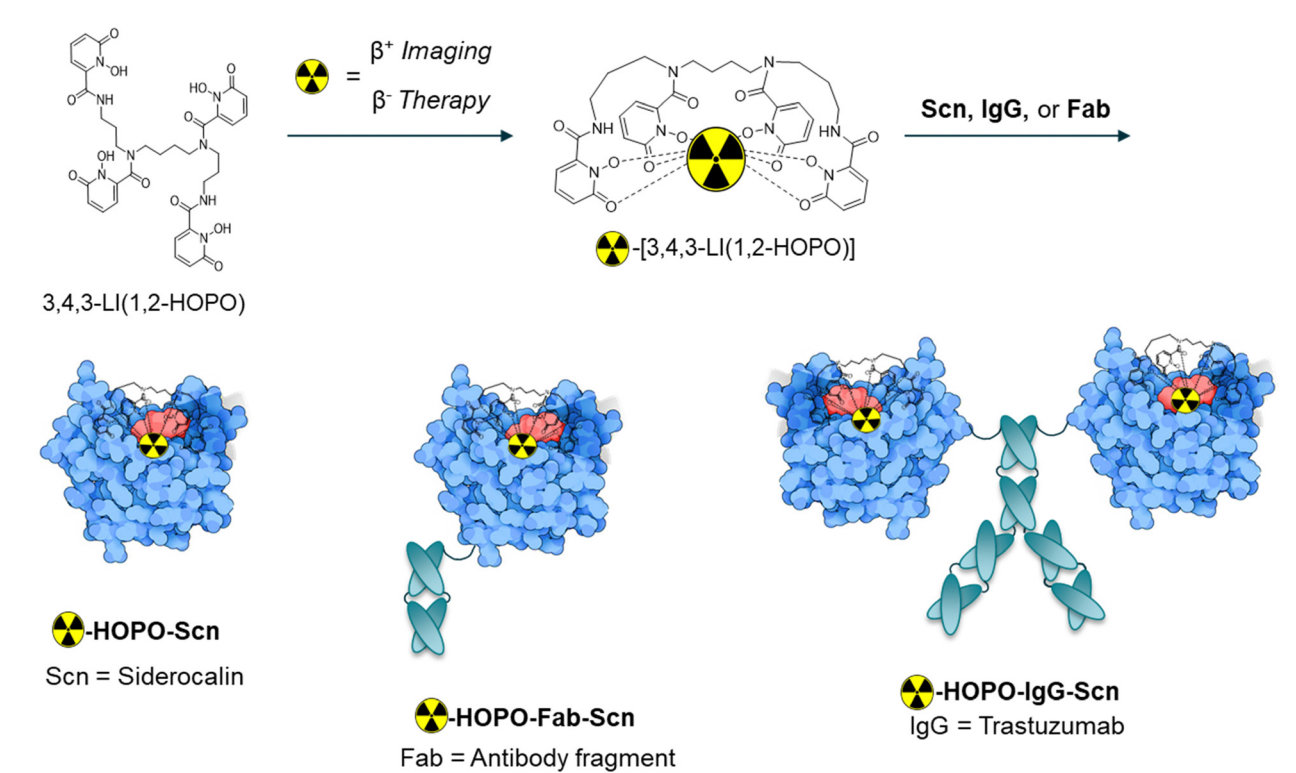


Fig. 1 Targeting fusion proteins explored in this work incorporate the Siderocalin (Scn) mammalian protein, which recognizes negatively charged M(III)-HOPO complexes (left, non-targeting control), and is fused either to an antibody fragment (Fab, middle) or trastuzumab (IgG, right).

Radio-TLC was used to determine radiochemical yields and construct stability (Table S2, Fig. S6-S9, ESI†). Radiochemical yields of 55-90% were obtained for labeled 86/90Y-HOPO-Scn. ^{86/90}Y-HOPO-Fab-Scn, and ^{86/90}Y-HOPO-IgG-Scn. In addition, monitoring of the protein constructs over 72 hours in PBS at room temperature indicated that the isotope stayed bound to the macromolecular fraction.

To evaluate the uptake of the trastuzumab and fragmentfunctionalized proteins, mice with SKOV-3 xenografts were injected intraperitoneally (I.P., 100 µCi, 0.2 mL) and subsequently imaged at 5, 25, and 50 hours post-injection (p.i.) on a Concorde microPET R4. Our previous in vivo imaging of the nontargeted 86Y-HOPO complex demonstrated rapid hepatic

clearance, visualized by uptake primarily in the gastrointestinal tract 15 minutes post-injection with complete clearance after 24 hours. With a similar amount of activity injected of 86Y, the images collected on the same PET scanner demonstrate comparable signal contrast.9 The diminished background signal could be attributed to the 75% emission of gamma-rays from ⁸⁶Y with energies between 200 and 3000 keV, which have the potential to scatter into the PET imaging window despite the 33% positron branching ratio. 19,20 Promisingly, for the nontargeting and targeting constructs, no bone or liver uptake was observed in the PET images after 50 hours, indicating the 86Y-HOPO protein constructs do not release yttrium in vivo (Fig. 2). Unfortunately, due to non-ideal tumor location on the

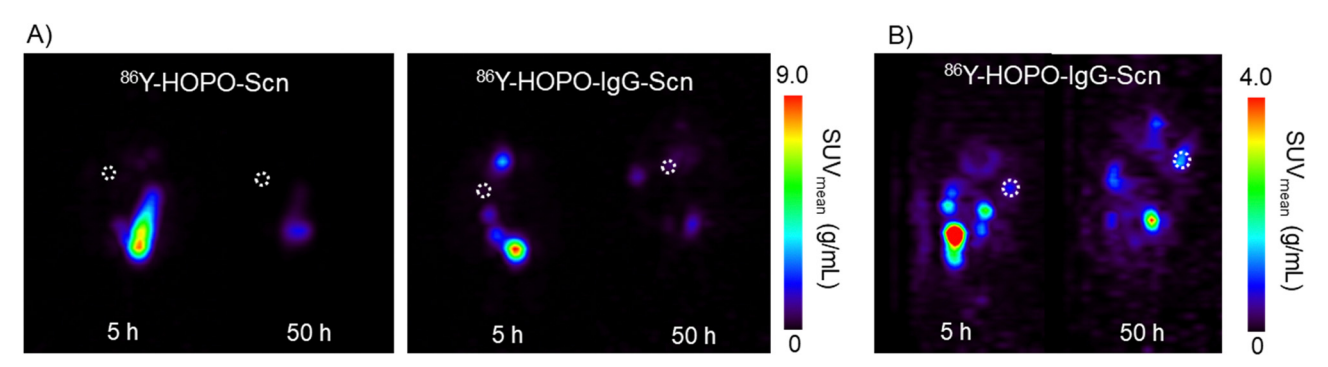


Fig. 2 (A) Coronal PET images (mouse lying prone, head at top) of targeting 86Y-HOPO-Scn (left) compared to 86Y-HOPO-IgG-Scn (right). (B) Sagittal view (mouse lying prone, head at top) showing tumor uptake. White dotted circle outlines tumor location. The most uptake is seen in the bladder at 5 h P.I. for both constructs

back/spine, distinct tumor uptake is difficult to distinguish in the coronal view, but taken together with the sagittal view, uptake was observed with 86Y-HOPO-IgG-Scn (Fig. 2, right). Although most activity is cleared renally through the kidneys and bladder, 2-fold increase in %ID is observed in the tumor after 25 hours and increased to a 3-fold increase in %ID at 50 hours. The gradual increase in uptake along with the renal excretion profile indicates strong in vivo stability. The nontargeting control, by contrast, is quickly excreted through the kidneys, with 76% of the injected dose cleared after 25 hours and 98% after 50 hours (Fig. S11, ESI†). However, minimal uptake was observed for the Fab-Scn fusion proteins, likely because the smaller antibody fragment is cleared too quickly before accumulating at the tumor site, a phenomenon observed in other antibody fragment systems²¹ (Fig. S11, ESI†). Further biodistribution studies were carried out by injecting 45 μCi (0.2 mL, I.P.) of 90Y-HOPO-IgG-Scn, 90Y-HOPO-Fab-Scn, and non-targeting 90Y-HOPO-Scn in addition to PBS as a control. Mice were euthanized 24 hours p.i. and organs of interest (liver, kidney, spleen, heart, lung, tumor, and remaining abdominal cavity) were harvested and processed for liquid scintillation counting (Fig. S12, ESI†). Similar to what was observed with the PET images, minimal ⁹⁰Y deposited in the bone or liver, further confirming no release of free yttrium from the ligand or ligandprotein construct. Instead, the conjugates are each cleared rapidly through the kidneys with minimal residual uptake after 24 hours according to LSC counting and by image analysis at 25 and 50 hours. Efforts are on-going to further establish Scn-IgG uptake in vitro and in vivo with other ligand and metal systems.

Conclusions

Here we report a rapid, room temperature radiolabeling method *via* ^{86/90}Y-HOPO incorporation into a targeting fusion protein. This opens directions for future fusion protein systems that take advantage of facile radiolabeling and formulation. The rapid non-covalent binding interaction between the negatively charged HOPO complexes and Scn fusion proteins could conceivably allow for purification-free, cold-kit labeling strategies ("mix-and-go"). However, this is the first demonstration of the applicability of fusion siderocalin proteins toward theranostic approaches. Future work aimed at developing a pretargeting system could improve targeting efficiency and potentially expand to further timepoints to account for longer trastuzumab circulation time.

Author contributions

Conceptualization: AGC, TAB, RKS, RJA; investigation: AGC, TA, TAB, MB, JJW, LMAQ, JVAV, JNW, ANG; data curation: AGC, TA, TAB, JVAV, RKS, RJA; writing – original draft: AGC; writing – review & editing: AGC, TA, TAB, MB, JJW, LMAQ, JVAV, JNW, ANG, RKS, RJA; funding acquisition: RKS, RJA.

Conflicts of interest

RJA and RKS are listed as inventors on patent applications filed by the Lawrence Berkeley National Laboratory (LBNL) and the Fred Hutchinson Cancer Center, describing inventions related to the research results presented here. The authors declare no competing financial interest.

Acknowledgements

All protocols and procedures used in the *in vivo* studies were reviewed and approved by the Institutional Animal Care and Use Committee of LBNL, and were performed in AAALAC accredited facilities, in compliance with guidelines from the Public Health Service's National Institutes of Health Office of Laboratory Animal Welfare. This work was supported by the University of California Contractor Supporting Research Program at LBNL under U.S. Department of Energy (DOE) Contract No. DE-AC02-05CH11231. We acknowledge additional support from the DOE, Office of Science, Office of Basic Energy Sciences, Chemical Sciences, Geosciences, and Biosciences Division at LBNL under Contract DE-AC02-05CH11231, for the spectroscopic characterization of metal-ligand-protein binding. We recognize the National Isotope Development Center managed by the DOE Isotope Program for supplying ⁸⁶Y.

References

- 1 R. Marcus, Use of ⁹⁰Y-Ibritumomab Tiuxetan in Non-Hodgkin's Lymphoma, *Semin. Oncol.*, 2005, **32**, 36–43, DOI: **10.1053/j.seminoncol.2005.01.012**.
- 2 R. Shannon, Revised Effective Ionic Radii and Systematic Studies of Interatomic Distances in Halides and Chalcogenides, Acta Crystallogr., Sect. A: Cryst. Phys., Diffr., Theor. Gen. Crystallogr., 1976, 32(5), 751–767, DOI: 10.1107/S0567739 476001551.
- 3 J. Dewulf, K. Adhikari, C. Vangestel, T. V. Wyngaert and F. Elvas, Development of Antibody Immuno-PET/SPECT Radiopharmaceuticals for Imaging of Oncological Disorders—An Update, *Cancers*, 2020, 12, 1868.
- 4 E. B. Ehlerding, C. A. Ferreira, E. Aluicio-Sarduy, D. Jiang, H. J. Lee, C. P. Theuer, J. W. Engle and W. Cai, ^{86/90}Y-Based Theranostics Targeting Angiogenesis in a Murine Breast Cancer Model, *Mol. Pharmaceutics*, 2018, **15**(7), 2606–2613, DOI: **10.1021/acs.molpharmaceut.8b00133**.
- 5 C. A. Ferreira, E. B. Ehlerding, Z. T. Rosenkrans, D. Jiang, T. Sun, E. Aluicio-Sarduy, J. W. Engle, D. Ni and W. Cai, 86/90Y-Labeled Monoclonal Antibody Targeting Tissue Factor for Pancreatic Cancer Theranostics, *Mol. Pharmaceutics*, 2020, 17(5), 1697–1705, DOI: 10.1021/acs.molpharmaceut. 0c00127.
- 6 I. Captain, G. J. P. Deblonde, P. B. Rupert, D. D. An, M.-C. Illy, E. Rostan, C. Y. Ralston, R. K. Strong and R. J. Abergel, Engineered Recognition of Tetravalent Zirconium and Thorium by Chelator-Protein Systems: Toward Flexible Radiotherapy and Imaging Platforms, *Inorg. Chem.*,

- 2016, 55(22), 11930-11936, DOI: 10.1021/acs.inorgchem. 6b02041.
- 7 L. D. Loomis and K. N. Raymond, Solution Equilibria of Enterobactin and Metal-Enterobactin Complexes, Inorg. Chem., 1991, 30(5), 906-911, DOI: 10.1021/ic00005a008.
- 8 R. J. Abergel, M. C. Clifton, J. C. Pizarro, J. A. Warner, D. K. Shuh, R. K. Strong and K. N. Raymond, The Siderocalin/Enterobactin Interaction: A Link between Mammalian Immunity and Bacterial Iron Transport, J. Am. Chem. Soc., 2008, 130(34), 11524-11534, DOI: 10.1021/ja803524w.
- 9 K. P. Carter, G. J. P. Deblonde, T. D. Lohrey, T. A. Bailey, D. D. An, K. M. Shield, W. W. Lukens and R. J. Abergel, Developing Scandium and Yttrium Coordination Chemistry to Advance Theranostic Radiopharmaceuticals, Commun. Chem., 2020, 3(1), 61, DOI: 10.1038/s42004-020-0307-0.
- 10 M. Sturzbecher-Hoehne, C. Ng Pak Leung, A. D'Aléo, B. Kullgren, A.-L. Prigent, D. K. Shuh, K. N. Raymond and R. J. Abergel, 3,4,3-LI(1,2-HOPO): In Vitro Formation of Highly Stable Lanthanide Complexes Translates into Efficacious in Vivo Europium Decorporation, Dalton Trans., 2011, 40(33), 8340-8346, DOI: 10.1039/C1DT10840A.
- 11 B. E. Allred, P. B. Rupert, S. S. Gauny, D. D. An, C. Y. Ralston, M. Sturzbecher-Hoehne, R. K. Strong and R. J. Abergel, Siderocalin-Mediated Recognition, Sensitization, and Cellular Uptake of Actinides, Proc. Natl. Acad. Sci. U. S. A., 2015, 112(33), 10342-10347, DOI: 10.1073/pnas.1508902112 (accessed 2023/01/09).
- 12 G. J. P. Deblonde, M. Sturzbecher-Hoehne and R. J. Abergel, Solution Thermodynamic Stability of Complexes Formed with the Octadentate Hydroxypyridinonate Ligand 3,4,3-LI(1,2-HOPO): A Critical Feature for Efficient Chelation of Lanthanide(IV) and Actinide(IV) Ions, Inorg. Chem., 2013, 52(15), 8805-8811, DOI: 10.1021/ic4010246.
- 13 M. Sturzbecher-Hoehne, B. Kullgren, E. E. Jarvis, D. D. An and R. J. Abergel, Highly Luminescent and Stable Hydroxypyridinonate Complexes: A Step Towards New Curium Decontamination Strategies, Chem. - Eur. J., 2014, 20(32), 9962-9968, DOI: 10.1002/chem.201402103(accessed 2023/ 01/09).
- 14 M. A. Deri, S. Ponnala, P. Kozlowski, B. P. Burton-Pye, H. T. Cicek, C. Hu, J. S. Lewis and L. C. Francesconi,

- p-SCN-Bn-HOPO: A Superior Bifunctional Chelator for 89Zr ImmunoPET, Bioconjugate Chem., 2015, 26(12), 2579-2591, DOI: 10.1021/acs.bioconjchem.5b00572.
- 15 P. J. Yazaki, T. Kassa, C.-W. Cheung, D. M. Crow, M. A. Sherman, J. R. Bading, A.-L. J. Anderson, D. Colcher and A. Raubitschek, Biodistribution and Tumor Imaging of an Anti-CEA Single-Chain Antibody-Albumin Fusion Protein, Nucl. Med. Biol., 2008, 35(2), 151-158, DOI: 10.1016/ j.nucmedbio.2007.10.010.
- 16 L. Cavina, D. van der Born, P. H. M. Klaren, M. C. Feiters, O. C. Boerman and F. P. J. T. Rutjes, Design of Radioiodinated Pharmaceuticals: Structural Features Affecting Metabolic Stability towards in Vivo Deiodination, Eur. J. Org. Chem., 2017, 3387-3414, DOI: 10.1002/ejoc.2016 01638(acccessed 2023/03/01).
- 17 A. D. Bandaranayake, C. Correnti, B. Y. Ryu, M. Brault, R. K. Strong and D. J. Rawlings, Daedalus: a Robust, Turnkey Platform for Rapid Production of Decigram Quantities of Active Recombinant Proteins in Human Cell Lines using Novel Lentiviral Vectors, Nucleic Acids Res., 2011, 39(21), e143, DOI: 10.1093/nar/gkr706 (accessed 4/1/2023).
- 18 C. E. Correnti, M. M. Gewe, C. Mehlin, A. D. Bandaranayake, W. A. Johnsen, P. B. Rupert, M.-Y. Brusniak, M. Clarke, S. E. Burke and W. De Van Der Schueren, et al., Screening, Large-Scale Production and Structure-Based Classification of Cystine-Dense Peptides, Nat. Struct. Mol. Biol., 2018, 25(3), 270-278, DOI: 10.1038/s41594-018-0033-9.
- 19 F. Rösch, H. Herzog and S. M. Qaim, The Beginning and Development of the Theranostic Approach in Nuclear Medicine, as Exemplified by the Radionuclide Pair 86Y and 90Y, Pharmaceuticals, 2017, 10, 56.
- 20 M. Le Fur and P. Caravan, Chapter Ten-86Y PET imaging, in Methods in Enzymology, ed. J. A. Cotruvo, Academic Press, 2021, vol. 651, pp. 313-342.
- 21 C. T. Mendler, L. Friedrich, I. Laitinen, M. Schlapschy, M. Schwaiger, H.-J. Wester and A. Skerra, High Contrast Tumor Imaging with Radio-Labeled Antibody Fab Fragments Tailored for Optimized Pharmacokinetics via PASylation, mAbs, 2015, 7(1), 96-109, DOI: 10.4161/19420862. 2014.985522.